Fermi National Accelerator Laboratory

FERMILAB-Pub-92/51-E
E665

Saturation of Shadowing at Very Low x_{Bj}

The E665 Collaboration

Fermi National Accelerator Laboratory
P.O. Box 500, Batavia, Illinois 60510

March 1992

Submitted to *Physical Review Letters*.

Operated by Universities Research Association Inc. under Contract No. DE-AC02-76CHO3000 with the United States Department of Energy

Disclaimer

Saturation of Shadowing at Very Low x_{Bj}

the Fermilab E665 collaboration

ABSTRACT

The ratio of cross sections for inelastic muon scattering on xenon and deuterium nuclei was measured at very low x_{Bj} ($0.00002 < x_{Bj} < 0.25$). The data were taken at Fermilab experiment E665 with a 490 GeV/c muon beam incident on liquid deuterium and gaseous xenon targets. Two largely independent analysis techniques gave statistically consistent results. The xenon–to–deuterium per–nucleon cross–section ratio is constant at approximately 0.7 for x_{Bj} below 0.003.

Submitted to Physical Review Letters

THE FERMILAB E665 COLLABORATION

M. R. Adams[6], S. Aïd[9], P. L. Anthony[10,a], M. D. Baker[10], J. Bartlett[4], A. A. Bhatti[13,b], H. M. Braun[14], W. Busza[10], T. J. Carroll[6], J. M. Conrad[5], G. Coutrakon[4,c], R. Davisson[13], I. Derado[11], S. K. Dhawan[15], W. Dougherty[13], T. Dreyer[1], K. Dziunikowska[8], V. Eckardt[11], U. Ecker[14,q], M. Erdmann[1,e], A. Eskreys[7], J. Figiel[7], H. J. Gebauer[11], D. F. Geesaman[2], R. Gilman[2,d], M. C. Green[2,f], J. Haas[1], C. Halliwell[6], J. Hanlon[4], D. Hantke[11], V. W. Hughes[15], H. E. Jackson[2], D. E. Jaffe[6,g], G. Jancso[11], D. M. Jansen[13,h], S. Kaufman[2], R. D. Kennedy[3], T. Kirk[4,i], H. G. E. Kobrak[3], S. Krzywdzinski[4], S. Kunori[9], J. J. Lord[13], H. J. Lubatti[13], D. McLeod[6], S. Magill[6,i], P. Malecki[7], A. Manz[11], H. Melanson[4], D. G. Michael[5,j], W. Mohr[1], H. E. Montgomery[4], J. G. Morfin[4], R. B. Nickerson[5,k], S. O'Day[9,l], K. Olkiewicz[7], L. Osborne[10], V. Papavassiliou[15,i], B. Pawlik[7], F. M. Pipkin[5,o], E. J. Ramberg[9,l], A. Röser[14,r], J. J. Ryan[10], A. Salvarani[3,m], H. Schellman[12], M. Schmitt[5,n], N. Schmitz[11], K. P. Schüler[15], H. J. Seyerlein[11], A. Skuja[9], G. A. Snow[9], S. Söldner-Rembold[11], P. H. Steinberg[9,o], H. E. Stier[1,o], P. Stopa[7], R. A. Swanson[3], R. Talaga[9,i], S. Tentindo-Repond[2,p], H.-J. Trost[2], H. Venkataramania[15], M. Vidal[11], M. Wilhelm[1], J. Wilkes[13], Richard Wilson[5], W. Wittek[11], S. A. Wolbers[4], T. Zhao[13]

[1] Albert-Ludwigs-Universität, D-7800 Freiburg i. Br., Germany
[2] Argonne National Laboratory, Argonne, Illinois 60439
[3] University of California, San Diego, California 92093
[4] Fermi National Accelerator Laboratory, Batavia, Illinois 60510
[5] Harvard University, Cambridge, Massachusetts 02138
[6] University of Illinois, Chicago, Illinois 60680
[7] Institute for Nuclear Physics, Krakow, Poland
[8] Institute for Nuclear Physics, Academy of Mining and Metallurgy, Krakow, Poland
[9] University of Maryland, College Park, Maryland 20742
[10] Massachusetts Institute of Technology, Cambridge, Massachusetts 02139
[11] Max–Planck–Institut für Physik, D-8000 Munich-40, Germany
[12] Northwestern University, Evanston, Illinois 60208
[13] University of Washington, Seattle, Washington 98195
[14] University of Wuppertal, D-5600 Wuppertal, Germany
[15] Yale University, New Haven, Connecticut 06511

[a] Present address: Lawrence Livermore National Laboratory, Livermore, California 94550

[b] Present address: The Rockefeller University, New York, New York 10021

[c] Present address: Loma Linda University Medical Center, Loma Linda, California 92350

[d] Present address: Rutgers University, Piscataway, New Jersey 08855

[e] Present address: DESY, Notkestr. 85, 2000 Hamburg, Germany

[f] Present address: LeCroy Research Systems, Spring Valley, New York 10977

[g] Present address: Laboratoire de l'Accélérateur Linéaire, 91405 Orsay, France

[h] Present address: Los Alamos National Laboratory, Los Alamos, New Mexico 87545

[i] Present address: Argonne National Laboratory, Argonne, Illinois 60439

[j] Present address: California Institute of Technology, Pasadena, California 91125

[k] Present address: Oxford University, Oxford, OX1 3NP United Kingdom

[l] Present address: Fermi National Accelerator Laboratory, Batavia, Illinois 60510

[m] Present address: A. T. & T, Bell Labs. 2000 North Naperville Road, Naperville, Illinois 60555

[n] Present address: University of Wisconsin, Madison, Wisconsin 53706

[o] Deceased

[p] Present address: Northern Illinois University, Dekalb, Illinois 60115

[q] Present address: Büro Schellmann, Rabenhorst 29, Hamburg 65, Germany

[r] Present address: Ruhruniversität Bochum, D-4630 Bochum 1, Germany

Shadowing, a depletion of the cross section per nucleon in heavy nuclei as compared to deuterium, has been observed in collisions of real and virtual photons with nuclei in several experiments [1, 2, 3, 4, 5]. These experiments showed that the ratio of the inelastic per–nucleon cross sections of heavy nuclei to deuterium decreases from unity as x_{Bj} decreases from 0.1 to 0.002 ($x_{Bj} = Q^2/2M\nu$ where Q^2 is the four–momentum squared, ν is the energy transfered in the lab from the muon to the target and M is the proton mass)[2, 3, 4, 5]. In addition the data at the lowest measured x_{Bj} tend toward the photoproduction data[1] on heavy nuclei, although no evidence for saturation has been observed in previous inelastic–scattering experiments. It was the aim of this experiment to investigate the behavior of the ratio of the xenon and deuterium per–nucleon cross sections down to x_{Bj} of 0.00002, two orders of magnitude lower than any previous experiment.

Fermilab experiment 665 has been described in detail elsewhere[6], only relevant features will be mentioned. A 490 GeV/c positive muon beam impinged upon either a liquid deuterium (15.5 g/cm^2, length = 115 cm) or pressurized xenon gas (8.5 g/cm^2, 113 cm) target located in the first of two analysis magnets. Charged tracks were momentum–analyzed with a series of wire chambers and muons were identified with four stations of proportional chambers and hodoscopes located behind a three–meter thick steel absorber. Essential to the extraction of the cross–section ratio at low x_{Bj} was the electromagnetic calorimeter. The calorimeter consisted of 20 lead–proportional tube layers (total thickness of 20 radiation lengths) with pad read–out giving a transverse position resolution of approximately 1 cm.

Figure 1 shows the event distributions as a function of x_{Bj} for the two targets after kinematic cuts. The kinematic cuts applied were $0.01 < Q^2 < 60(GeV/c)^2$, $\nu > 40$ GeV, $y < 0.90$, $E_{BEAM} > 400$ GeV and $|\phi_{\mu'} - \pi| > 0.2$ where E_{BEAM} is the incident muon energy,

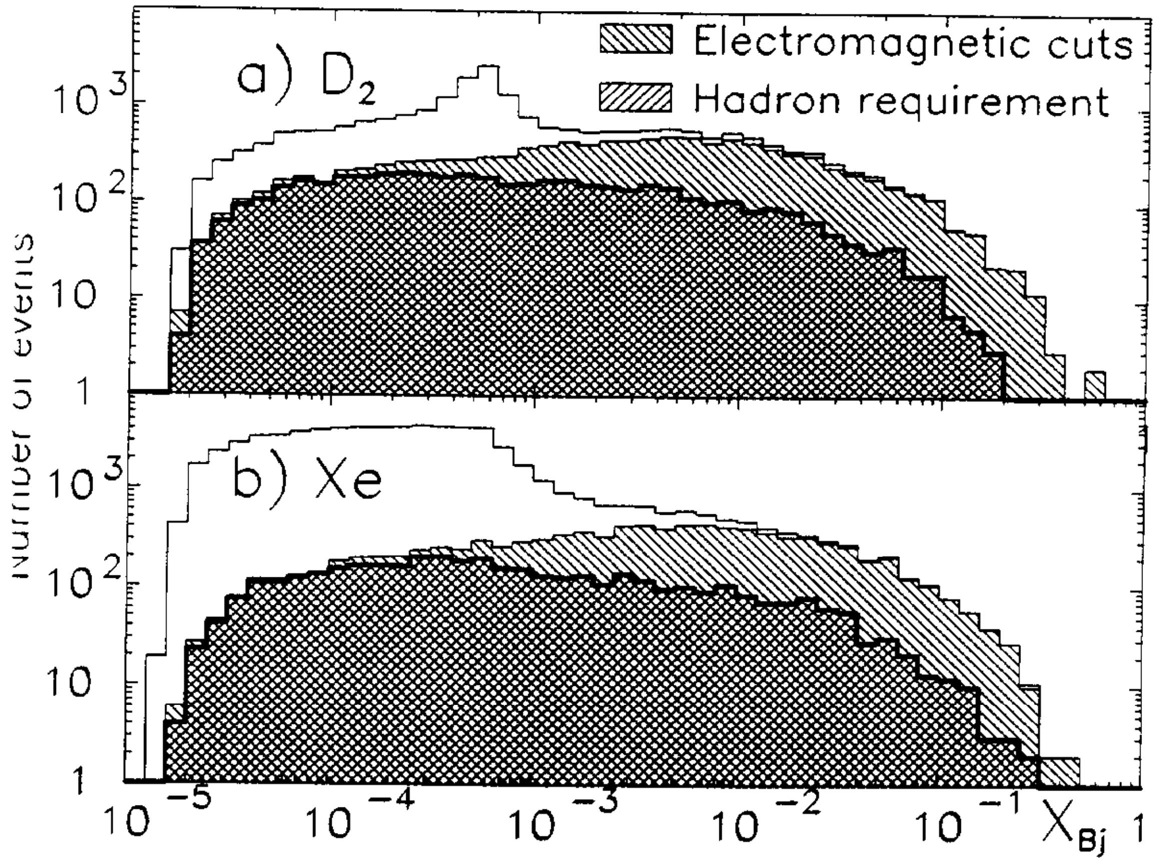

Figure 1: The number of events from the a)deuterium and b) xenon targets *versus* x_{Bj} is shown. The solid histogram shows the distributions after the application of the kinematic cuts and the diagonally–striped histograms show the distributions after the electromagnetic cuts or hadron requirement.

$y \equiv \nu/E_{BEAM}$, and $\phi_{\mu'}$ is the azimuthal angle of the scattered muon around the direction of the incident muon relative to the horizontal midplane of the analyzing magnet. The Q^2 and ν cuts limit the data to regions where the resolution in x_{Bj} is $\leq 60\%$, the y cut reduces contamination by radiative, quasi–elastic and coherent scattering events, and the cut on the azimuthal angle of the scattered muon eliminates muons that interacted downstream of the target but were incorrectly reconstructed as having an interaction vertex in the target.

Significant electromagnetic backgrounds survive the kinematic cuts, as is apparent in figure 1. The peak at $x_{Bj} = M_{electron}/M_{proton}$, clearly visible in the deuterium data, is due to elastic muon–electron (μe) scattering, while the large broad peak in the xenon data results mainly from radiative coherent muon–nucleus scattering ($\mu\gamma$). To separate the inelastic scattering events from these large backgrounds, two largely independent and complementary techniques were employed — the "hadron requirement" and the "electromagnetic cuts". The techniques are not completely independent because each requires that the scattered muon be reconstructed.

To satisfy the hadron requirement, an event was required to have at least two positive tracks, not including the scattered muon, or at least two negative tracks fitted to the interaction vertex. This requirement, essentially a multiplicity cut, explicitly excludes elastic μe scatters and electron pair production in the target and implicitly assumes that relatively high multiplicity events are due to inelastic scattering[8].

Conversely, the electromagnetic cuts were based on the hypothesis that each event was due to $\mu\gamma$ or μe elastic scattering. An event was rejected as due to $\mu\gamma$ if the total calorimeter energy was greater than 0.45ν or if there was an energy deposit in the calorimeter that was coplanar with the incoming– and scattered–muon vectors[9]. Elastic μe scatters were rejected by an energy–dependent cut on the distance between the predicted calorimeter impact position of a hypothesized electron trajectory and a calorimeter energy deposit. The hypothesized electron trajectory was calculated from the incoming– and scattered–muon vectors by assuming an elastic μe collision had occurred at the reconstructed muon–scattering vertex.

Figure 1 shows the resulting distribution of events after the application of cuts for the xenon and deuterium data. Both the hadron requirement and the electromagnetic cuts greatly reduce the number of events at low x_{Bj} . As x_{Bj} increases (decreasing ν), the number of events satisfying the hadron requirement decreases as expected from a multiplicity cut. The distribution of events passing the electromagnetic cuts is consistent with that of the events passing the hadron cuts at low x_{Bj} and makes a smooth transition to that of the events passing the kinematic cuts as x_{Bj} increases into the range where the electromagnetic backgrounds are small.

The xenon and deuterium data were taken during separate running periods resulting in a relative reconstruction efficiency factor of 1.04 applied to the Xe/D_2 cross–section ratio with an estimated limit of systematic uncertainty of ± 0.07[4]. Triggering efficiencies during the two running periods were identical to within an estimated $\pm 1\%$ systematic uncertainty. In addition a correction (<2%) was applied for the 5% contamination by volume of the "deuterium" target with HD[10]. The measurement precision of the target densities contributed an additional $\pm$ 0.5% systematic uncertainty to the cross–section ratio. No acceptance corrections have been applied to the ratio.

Inelastic scattering without shadowing, bremsstrahlung and muon–electron elastic collisions were simulated by a Monte Carlo which modelled the response of the apparatus and secondary interactions in the detector.

The Xe/D_2 cross–section ratio determined by subjecting Monte Carlo inelastic–scattering events to the same analysis techniques was statistically consistent with unity as a function of x_{Bj} ,Q^2 and ν. The distribution of this Monte Carlo Xe/D_2 inelastic–scattering cross–section ratio about unity was used to estimate a conservative, overall limit of systematic uncertainty of the two techniques of $\pm 6.5\%$.

In addition the data analysis technique was varied to obtain an estimate of the x_{Bj}–dependence of the systematic uncertainty. Included in the comparison were A) a variation of the $\mu\gamma$ cut by 10%, B) a more restrictive cut on the resolution in x_{Bj} , C) the use of the kinematics from the vertex determined by the incident and scattered muon only, and D) a cut on the primary vertex well within the endcaps of the target vessels.

Studies of the bremsstrahlung and muon–electron Monte Carlos showed that the amount of electromagnetic background that remained after the electromagnetic cuts(hadron requirement) was less than 5%(15%) in the Xe/D_2 cross–section ratio for $x_{Bj} < 0.003$ and negligible above 0.003. An x_{Bj}–dependent correction for this effect has been applied to the cross–section ratio.

Thus, there are two components to the estimated systematic uncertainty:

1. An x_{Bj}–dependent part representing the limit of uncertainty arising from the electromagnetic background subtraction and from the behavior of the Xe/D_2 cross–section ratio when the analysis technique was varied.

2. An x_{Bj}–independent, overall systematic uncertainty of $\pm 10\%$ arising mainly from the $\pm 6.5\%$ relative normalization uncertainty and the estimated $\pm 6.5\%$ uncertainty derived from the Monte Carlo Xe/D_2 cross–section ratio.

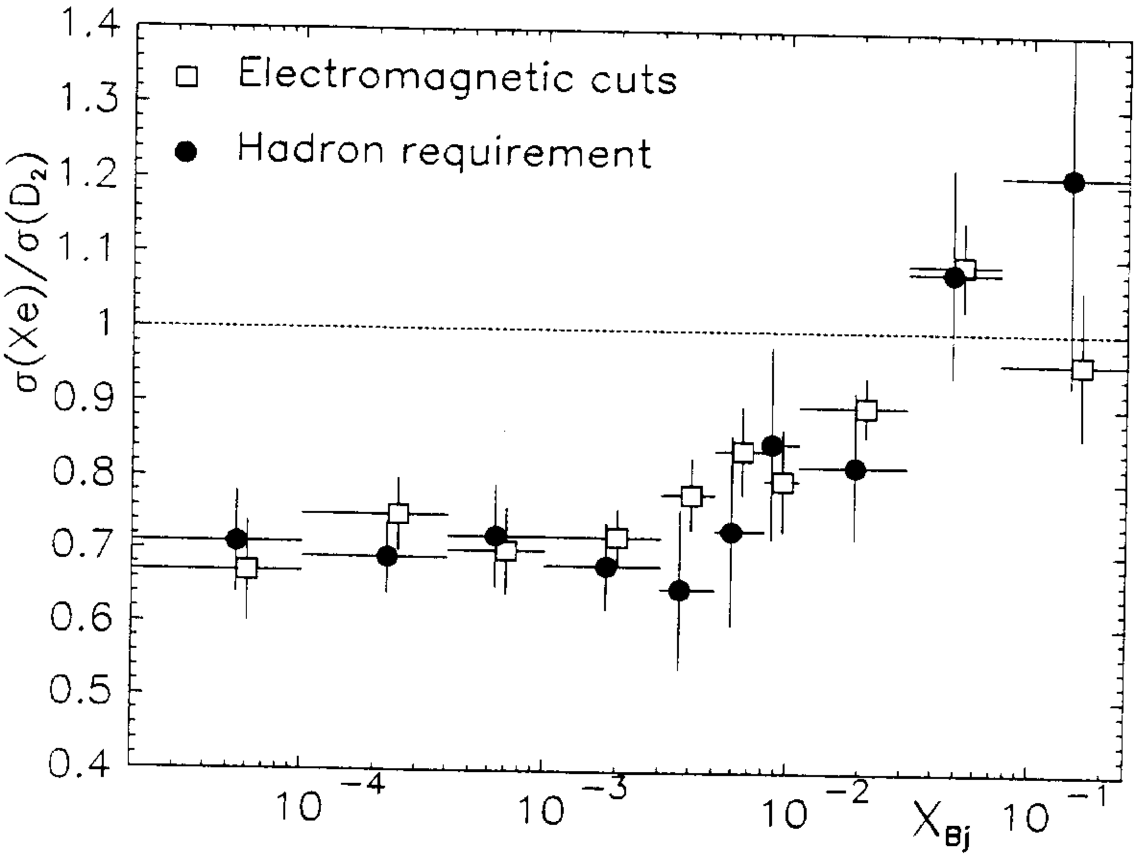

Figure 2: The ratio of the xenon and deuterium per–nucleon cross sections *versus* x_{Bj} as determined by the two analysis methods. The horizontal error bars show the bin width and the vertical error bars show the statistical uncertainty only. The ratio determined by the hadron requirement is displaced in x_{Bj} to make it easier to see the vertical error bars.

The two analysis techniques are compared in figure 2 which shows the Xe/D_2 per-nucleon cross-section ratio as a function of x_{Bj} . The two techniques yield statistically consistent results. In table 1 the results of the two analysis techniques are given with the average Q^2 for each x_{Bj} bin and the statistical and systematic uncertainties.

In figure 3 the E665 Xe/D_2 cross-section ratio measured with the statistically more precise results of the electromagnetic cuts is compared with the results of NMC[5] for the helium- , carbon- , and calcium-deuterium ratios and the photoproduction results[1] interpolated to a xenon target and extrapolated to $\nu = 150$ GeV. The A-dependence of shadowing measured in NMC is consistent with the results shown here within the systematic uncertainty shown and the quoted $\approx 1\%$ systematic uncertainty for NMC. For x_{Bj} below 0.003, the Xe/D_2 ratio determined with the electromagnetic cuts[hadron requirement] is constant at $0.72 \pm 0.03(\text{stat.}) \pm 0.07(\text{syst.})$ $[0.70 \pm 0.03(\text{stat.}) \pm 0.07(\text{syst.})]$, and indicates a saturation in shadowing at very low x_{Bj} . The saturation value is also consistent with the photoproduction point at 0.60 ± 0.03, derived for γ-Xe scattering [11].

In summary E665 has studied shadowing by measuring the inelastic Xe/D_2 per-nucleon cross-section ratio in the range $0.00002 < x_{Bj} < 0.25$ using two largely independent analysis techniques. The ratio saturates below $x_{Bj} = 0.003$ at $\sigma(Xe)/\sigma(D_2) \approx 0.7$.

Heartfelt gratitude goes to the personnel at Fermilab and at the participating institutions. This work was supported in part by the National Science Foundation, the U. S. Department of Energy and the Bundesministerium für Forschung and Technologie.

x_{Bj} bin	$\langle Q^2 \rangle$ $(GeV/c)^2$	$\sigma(Xe)/\sigma(D_2)$ Electromagnetic cuts	Hadron requirement
0.00002–0.0001	0.03	0.67±0.07±0.05	0.71±0.07±0.08
0.0001–0.0004	0.10	0.75±0.05±0.06	0.69±0.05±0.11
0.0004–0.001	0.23	0.70±0.06±0.11	0.72±0.07±0.16
0.001–0.003	0.50	0.72±0.04±0.05	0.68±0.06±0.06
0.003–0.005	0.89	0.78±0.05±0.04	0.65±0.11±0.04
0.005–0.008	1.34	0.84±0.06±0.03	0.73±0.13±0.03
0.008–0.011	1.91	0.80±0.07±0.02	0.85±0.13±0.02
0.011–0.031	3.58	0.90±0.04±0.05	0.82±0.10±0.05
0.031–0.075	8.20	1.09±0.06±0.07	1.08±0.14±0.07
0.075–0.25	17.9	0.96±0.10±0.09	1.21±0.28±0.09

Table 1: The xenon–deuterium cross–section ratio obtained by the two analysis techniques with the statistical and x_{Bj} –dependent limit of systematic uncertainties, respectively. The overall systematic uncertainty of ±10% is not explicitly included in the table.

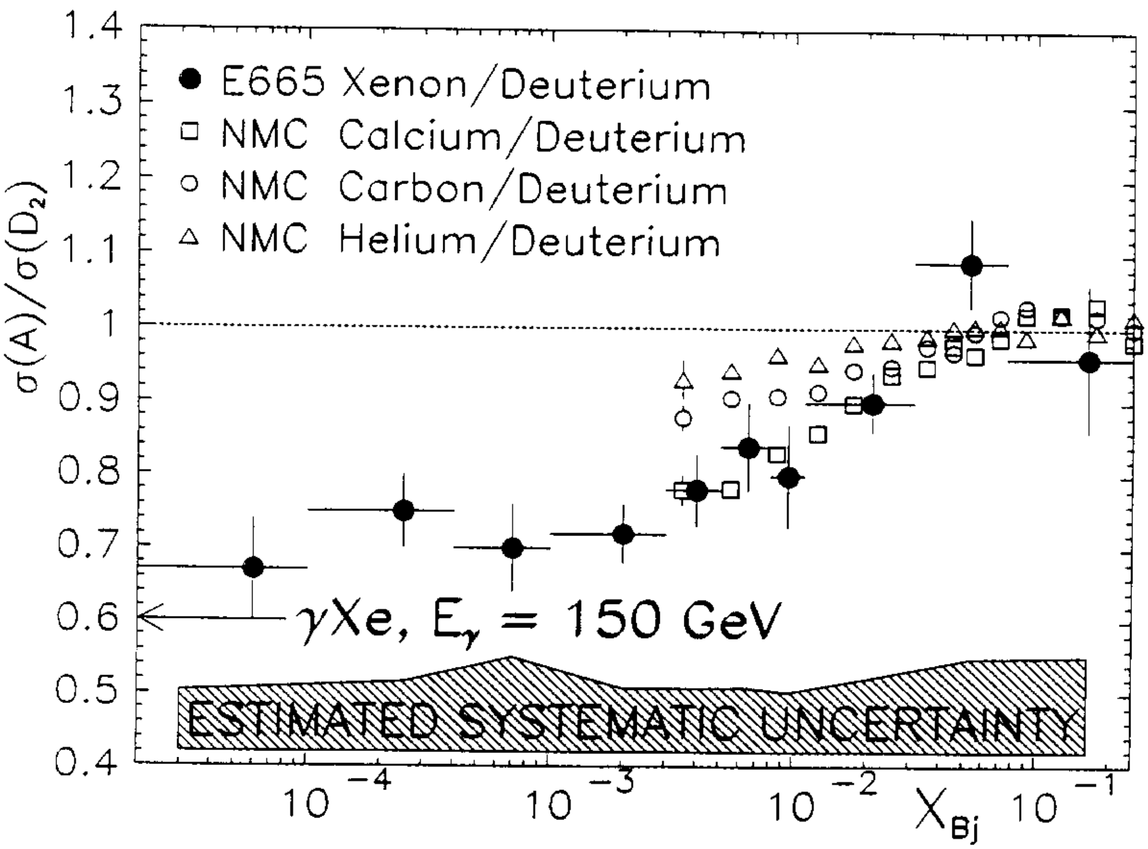

Figure 3: The ratio of the xenon and deuterium per–nucleon cross sections measured using the electromagnetic cuts is compared with the results of the NMC[5] for helium, carbon and calcium targets and a photoproduction experiment[1] interpolated to a xenon target and extrapolated to a photon energy of 150 *GeV*. The width of the shaded band represents the estimated systematic uncertainty of the E665 result with the x_{Bj}–dependent and ±10% overall systematic uncertainty added in quadrature.

References

[1] D.O. Caldwell *et al.*, Phys. Rev. Lett. **42**, 553 (1979).

[2] D.M. Alde *et al.*, Phys. Rev. Lett. **64** 2479 (1990).

[3] M. Arneodo *et al.*, Phys. Lett. **B333**, 1 (1990); M. Arneodo *et al.*, Phys. Lett. **B211**, 493 (1988).

[4] M.R. Adams *et al.*, E665 collaboration, FNAL 92/50-E, submitted to Physics Letters.

[5] P. Amaudruz et al., Z. Phys. **C51**, 387 (1991)

[6] M.R. Adams *et al.*, Nucl. Inst. and Meth. **A291** 533 (1990); M.R. Adams *et al.*, Phys. Lett. **B272**, 163 (1991).

[7] S.R. Magill, Ph.D. dissertation, 1990, Univ. of Illinois at Chicago (unpublished).

[8] A similar analysis technique is described in J. Eickmeyer *et al.*, Phys. Rev. Lett. **36**, 289 (1976).

[9] M.S. Goodman *et al.*, Phys. Rev. Lett. **47**, 293 (1981) also used electromagnetic calorimetry to differentiate bremsstrahlung and inelastic scattering processes.

[10] S. Aïd, Ph.D. dissertation, 1991, Univ. of Maryland (unpublished).

[11] The quoted value and uncertainty of the photoproduction point (0.60 ± 0.03) results from the propagation of the statistical errors of the data through the A–dependent and energy–dependent fits used to interpolate and extrapolate to a xenon target at a photon energy of 150 GeV.